Heralding Two-Photon and Four-Photon Path Entanglement on a Chip

Jonathan C. F. Matthews, Alberto Politi, Damien Bonneau, and Jeremy L. O'Brien*

Centre for Quantum Photonics, H. H. Wills Physics Laboratory & Department of Electrical and Electronic Engineering, University of Bristol, Merchant Venturers Building, Woodland Road, Bristol, BS8 1UB, United Kingdom

(Received 13 April 2011; revised manuscript received 17 August 2011; published 11 October 2011)

Generating quantum entanglement is not only an important scientific endeavor, but will be essential to realizing quantum-enhanced technologies, in particular, quantum-enhanced measurements with precision beyond classical limits. We investigate the heralded generation of multiphoton entanglement for quantum metrology using a reconfigurable integrated waveguide device in which projective measurement of auxiliary photons heralds the generation of path-entangled states. We use four and six-photon inputs, to analyze the heralding process of two- and four-photon NOON states—a superposition of N photons in two paths, capable of enabling phase supersensitive measurements at the Heisenberg limit. Realistic devices will include imperfections; as part of the heralded state preparation, we demonstrate phase superresolution within our chip with a state that is more robust to photon loss.

DOI: 10.1103/PhysRevLett.107.163602 PACS numbers: 42.50.Ex, 03.67.Bg, 06.20.−f

Quantum entanglement is understood to lie at the heart of proposed quantum technologies [1–3]. Entangling interactions between photons can be achieved using only linear optical circuits, additional photons, and photon detection [4,5] where a particular detection event heralds the success of a given process. In this way it is possible to generate multiphoton entangled states and indeed to efficiently perform universal, fault tolerant quantum computing [4]. There have been several examples of heralding two-photon [6–10] and four-photon [11] polarization entanglement for quantum information processing applications. In the context of quantum metrology, however, generating path-number entangled states (including "NOON" states) is a particularly important example where an N-photon entangled state is heralded from $>N$ input photons and several schemes for doing this have been proposed [12–14]. Here we use an integrated waveguide device to implement a scalable scheme for heralding path-entangled states of up to four photons, including ones which are robust to losses. This scheme scales to arbitrary N [15].

Subwavelength sensitivity makes optical interferometry one of the most powerful precision measurement tools available to modern science and technology [16], with applications from microscopy to gravity wave detection [17,18]. However, the use of classical states of light limits the phase precision $\Delta\theta$ of such measurements to the shot noise, or standard quantum limit (SQL): $\Delta\theta \cong 1/\sqrt{N}$, where N is the average number of sensing photons passing through the measurement apparatus. Quantum states of light—entangled states of photon number across the two paths of an interferometer for example—enable precision better than the SQL [3]. Quantum metrology promises to be of critical importance for applications where properties of the measured sample are altered by the sensing process: by using entangled light, the same level of precision in measurement can be achieved by exposing the sample to fewer photons. Conversely, for the same disturbance of the sample (i.e., the number of photons it is exposed to) more information can be extracted.

Entangled states of $M + N$ photons across two optical modes x and y of the form

$$|N :: M\rangle_{x,y}^{\alpha} = \frac{1}{\sqrt{2}}(|N\rangle_x|M\rangle_y + e^{i\alpha}|M\rangle_x|N\rangle_y) \quad (1)$$

can be used to increase the frequency of interference fringes by a factor of $|N - M|$ and to increase precision. The canonical example is the NOON state ($M = 0$), which enables the ultimate precision $\Delta\theta \cong 1/N$—the Heisenberg limit [19]. While NOON states are fragile with respect to photon loss, other linear superpositions of photon number entanglement can beat the SQL in interferometers with loss: states with $M \neq N$ are optimal for balanced loss [20]. Realistic application of these entangled states, however, demands a scalable and practical means of generating large $|N :: M\rangle$ states.

Multiphoton interference has been observed with postselection of three- [21], four- [22,23], and five-photon [24] states. To take advantage of the benefits of quantum metrology—whereby more information can be extracted for the same light intensity (photon flux through the sample) as a classical measurement—requires a scheme where the postselection probability is sufficiently high [25]. To obtain the maximum precision, however, postselection should be avoided, requiring either a deterministic or a heralded [12–15] method for generating high fidelity, large photon number $|N :: M\rangle_{x,y}^{\alpha}$ states. In general, this requires auxiliary photons and photon detection [4,15]. A heralding scheme to generate NOON state of polarization entangled photons has been demonstrated for up to three photons [26]. It is important to note that a heralding signal enables gating with an optical switch to expose the sample only to photons in the state $|N :: M\rangle_{x,y}^{\alpha}$; the rate of

production is given by the heralding probability but does not affect sensitivity.

For many precision measurement applications it is also important that the entangled state be encoded in two spatial modes (rather than polarization modes). Stability required for such encoding can be readily achieved in compact integrated quantum photonic devices [27], as demonstrated by two- [28,29] and four-photon [28] interference. While it is relatively straightforward to convert polarization entanglement to path entanglement in the bulk optical architecture, conversion is not so straightforward in the integrated optical architecture which, with the integration of photon sources and detectors, is of critical importance in bringing practical quantum technologies out of the research lab and into application.

The silica-on-silicon waveguide circuit shown in Fig. 1(a) is capable of heralding the two- and four-photon NOON states $|2::0\rangle_{j,k}^{0}$ and $|4::0\rangle_{j,k}^{\pi}$, as well as the four-photon state $|3::1\rangle_{j,k}^{0}$, dependent upon the input state and the setting of the internal phase ϕ, as we now explain. The circuit consists of directional couplers DC_{1-4}, equivalent to beam splitters with lithographically defined reflectivity η, used to couple photons between optical modes and for quantum interference [27]. The resistive heating element controls the relative optical phase ϕ inside the device. The state $|2::0\rangle_{j,k}^{0}$ can be generated by inputting four frequency degenerate photons, via polarization maintaining fiber (PMF), in the (unentangled) path encoded state $|2\rangle_b|2\rangle_c$. Quantum interference at the first directional coupler DC_1—designed to have a reflectivity $\eta = 0.5$—generates a superposition of the components $|4\rangle_e|0\rangle_f$, $|2\rangle_e|2\rangle_f$, and $|0\rangle_e|4\rangle_f$. After DC_3 and DC_4 this state evolves to a superposition across the four modes i, g, h, and l. However, only the component $|2\rangle_e|2\rangle_f$ gives rise to terms that include $|1\rangle_i|1\rangle_l$. Detecting one and only one photon in each of these two heralding modes therefore projects the quantum state across modes g and h to $|1\rangle_g|1\rangle_h$. Quantum interference [30] at the final directional coupler DC_2 yields the two-photon state $|2::0\rangle_{j,k}^{0}$. Provided DC_3 and DC_4 are $\eta = 0.5$, the intrinsic heralding success rate, i.e., the probability of detecting $|1\rangle_i|1\rangle_l$ and thereby heralding $|2::0\rangle_{j,k}^{0}$, is 1/16 (Ref. [12], see Supplemental Material [31]).

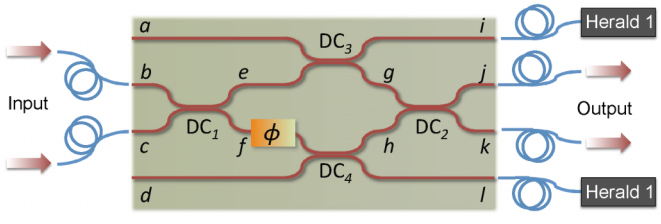

FIG. 1 (color online). Heralding multiphoton path-entangled states in a photonic chip. The waveguide circuit with coupling reflectivities $DC_{1,2} = 1/2$, $DC_{3,4} = 1/3$.

For a low loss regime and in the absence of higher-photon number terms, the heralding of the $|1\rangle_i|1\rangle_l$ component eliminates the lower order input state $|1\rangle_b|1\rangle_c$. We note that the requirements of heralding states for quantum metrology are more relaxed than for quantum computation or cryptography. A false heralded event of the vacuum state (due, for example, to a lower order input state $|1\rangle_b|1\rangle_c$) would be detrimental for any computation. In contrast, when low photon flux is the main requirement (exposure of a measured sample to radiation is to be kept to a minimum), a false heralding event of a vacuum state will not expose the sample to radiation.

The four-photon states $|3::1\rangle_{g,h}^{2\phi}$ and $|4::0\rangle_{j,k}^{\pi}$ are heralded in a similar manner: On inputting the state $|3\rangle_b|3\rangle_c$ of six frequency degenerate photons into the chip, nonclassical interference at DC_1 yields a coherent superposition of the components $|6\rangle_e|0\rangle_f$, $|4\rangle_e|2\rangle_f$, $|2\rangle_e|4\rangle_f$, and $|0\rangle_e|6\rangle_f$. On detecting one photon in each of the two modes i and l (again via DC_3 and DC_4) projects the state into a superposition state $|3::1\rangle_{g,h}^{2\phi}$. With the phase set to $\phi = 0$, the state returns to $|3::1\rangle_{j,k}^{0}$ after quantum interference at DC_2. With the phase set to $\phi = \pi/2$, however, quantum interference at DC_2 yields the four-photon NOON state $|4::0\rangle_{j,k}^{\pi}$. For $\eta = 0.5$ for both DC_3 and DC_4, the success rate of heralding $|4::0\rangle_{j,k}^{\pi}$ at the output is 3/64 (Ref. [12], see Supplemental Material [31]). Detection of the state $|4\rangle_j|0\rangle_k$, for example, leads to an interference fringe as a function of ϕ, with resolution double that of classical light, providing an important means of testing the required quantum coherence within the optical circuit with respect to the heralding scheme.

Four- and six-photon input states were generated using a bulk optical 785 nm, type-I pulsed down-conversion source (see Supplemental Material [31]) and coupled into the chip using polarization maintaining fiber. Detection of multiple photon states at the output of the chip in the same optical mode is accomplished nondeterministically using cascaded nonnumber resolving, optical fiber-coupled single-photon counting modules (SPCM, see Supplemental Material [31]). The heralding process is tested with the assumption of conservation of photon number at all of the outputs of the device coupled to the SPCM detection scheme; using number resolving detectors at outputs i and l, together with a deterministic photon source, would herald the generated entanglement without the need for counting all photons at the output of the device.

The phase instability of states leaving outputs j and k into a fiber or bulk optical circuit prevents a standard tomographic approach to reconstruct the density matrix of the state outside the chip. Development for an integrated optical quantum metrology device will incorporate the heralding circuit in one monolithic chip with all necessary components, including forming a waveguide interferometer for measuring unknown phase [28]. To analyze the

isolated circuit, we have employed a series of steps to test the coherence and measure the relative photon number of the output state of the chip: (i) Temporal coherence of the multiphoton input states were verified with a generalized Hong-Ou-Mandel experiment to observe quantum interference of the state $|2\rangle_b|2\rangle_c$ incident on a 50% reflectivity beam splitter—we observed $V = 34 \pm 4\%$ visibility interference in detecting two photons in each output of the beam splitter which, compared to the ideal $V = 1/3$ visibility, indicates temporal coherence of the multiphoton states generated in the photon source [23]; (ii) photon number statistics were measured at the outputs j and k (equivalent to the diagonal of the density matrix) using nondeterministic number resolving detection with optical fiber splitters; (iii) the output state was then interfered on a second beam splitter using a directional coupler inside the chip, via an inherently phase-stable fiber Sagnac loop.

The photon number statistics measured from the heralded two-photon NOON state at outputs j and k is plotted in Fig. 2(a). Probability-theoretic fidelity ($F = \sum_j \sqrt{p_j^e p_j^m}$) between the measured probability distribution (p^m) of photon statistics and the expected distribution (p^e) for the ideal state $|2 :: 0\rangle_{j,k}^0$ (also plotted) is $F_i = 0.95 \pm 0.01$. For $\lambda = 785$ nm operation, the reflectivities of DC_1 and DC_2 are measured to be $\eta = 0.542$ and 0.530, respectively. Using these measured reflectivities, and assuming otherwise perfect quantum interference, the expected output state was simulated; the fidelity between the photon number distribution of this simulated state and the experimental results is $F_s = 0.96 \pm 0.01$, leaving the discrepancy with perfect fidelity attributed to six- and higher-photon number terms from the down-conversion process and residual distinguishability of photons and not the device itself.

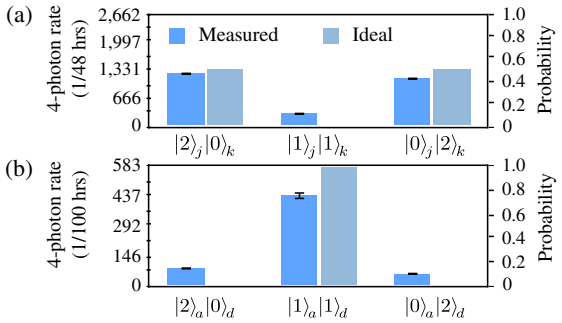

FIG. 2 (color online). Heralded $|20\rangle + |02\rangle$ state. (a) Measurement of photon statistics of the heralded two-photon NOON state. (b) Testing coherence of the heralded two-photon NOON state by measuring the photon statistics after nonclassical interference at DC_2 via a fiber Sagnac loop. Both distributions are normalized using single-photon detection rates to account for relative detector scheme, source, and waveguide coupling efficiencies. Error bars are given the standard deviation of detected events, assuming Poissonian statistics.

To test the coherence of the output of the circuit we formed a Sagnac loop by joining two optical fibers coupled to modes j and k (see Supplemental Material [31]). This configuration results in quantum interference at DC_2 in the reverse direction and is equivalent to interference at a separate beam splitter with zero relative optical phase of the two paths, fixed by the inherently stable Sagnac interferometer. By coupling detectors to waveguides a and d, the photon statistics of the quantum state returning through the chip after DC_2 at g and h can be measured, with an intrinsic loss due to $DC_{3,4}$. The fidelity between the measured distribution of photon statistics [Fig. 2(b)] and the one expected from a perfect $|2 :: 0\rangle_{j,k}^0$ state interfering at directional coupler DC_2 is $F_i = 0.90 \pm 0.03$. (Taking into account only the measured reflectivities of DC_1 and DC_2 the simulated detection rates agree with the experimental measurements with fidelity $F_s = 0.97 \pm 0.03$.) Together with the temporal coherence of the input and the high fidelity of the output state in the diagonal basis, this demonstrates coherence of the $|2 :: 0\rangle_{e,f}$ state.

Although Fig. 2(b) demonstrates coherence of the output state, the four-photon process that generates it does not rely on phase stability within the interferometer structure of the device. In contrast, heralding the $|4 :: 0\rangle_{j,k}^0$ state from the six-photon input state $|3\rangle_b|3\rangle_c$ requires coherent generation of the state $|3 :: 1\rangle_{g,h}^0$ within the interferometer. To test this coherence we injected the state $|3\rangle_b|3\rangle_c$ into the chip and sequentially set the phase to the four values $\phi = \pi/2$, π, $3\pi/2$, 2π. On detection of the six-photon state $|1\rangle_i|4\rangle_j|0\rangle_k|1\rangle_l$, we observed the sampled interference pattern plotted in Fig. 3(b) which demonstrates twofold superresolution compared to the single-photon interference pattern plotted in Fig. 3(a), and coherence of the state $|3 :: 1\rangle_{g,h}^0$ for subsequent generation of the $|4 :: 0\rangle_{j,k}^0$ state. The small number of data points does not allow fitting to a sinusoidal fringe. Note that $|3 :: 1\rangle_{g,h}^0$ is maximally entangled and is reported to be more robust to balanced loss, than the four-photon NOON state [20].

Figure 4 shows the photon statistics of the $|4 :: 0\rangle_{j,k}^0$ state that results from the quantum interference of the state $|3 :: 1\rangle_{g,h}^{\pi/2}$ at DC_2. We fixed the phase within the chip to $\phi = \pi/2$ and again injected the six-photon state $|3\rangle_b|3\rangle_c$ into the chip. Six photons were detected in all possible four-photon combinations on outputs j and k, together with a single photon in each of the heralding modes i and l. The fidelity between the resulting distribution of photon statistics and the distribution expected from measuring the ideal state $|4 :: 0\rangle_{j,k}^0$ is $F_i = 0.89 \pm 0.04$. Taking into account the measured reflectivities of DC_1 and DC_2, the simulated statistics agree with experimental measurements with a fidelity $F_s = 0.93 \pm 0.04$. The remaining discrepancy is attributed to a degree of distinguishability of the input photons—leading to imperfect quantum interference—and eight- and higher-photon number states from the

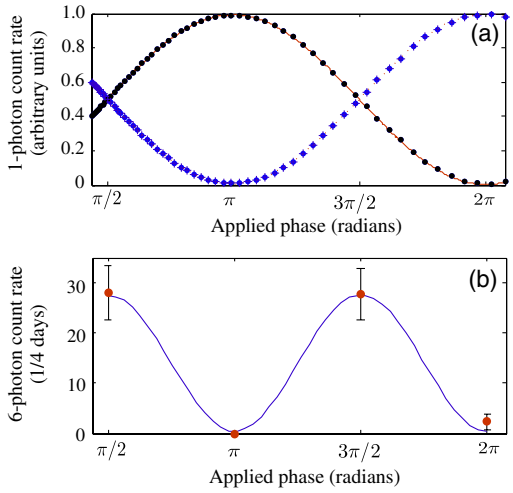

FIG. 3 (color online). Superresolution with a heralded four-photon entangled state. (a) Single-photon fringes from inputting light into waveguide b and varying the phase ϕ, displaying the expected pattern arising from classical interference pattern with period 2π. Black circles and blue diamonds, respectively, represent the normalized single photons count rate detected at output j and k. (b) The increased resolution interference pattern of manipulating ϕ of the state $|3::1\rangle_{e,f}^{\phi}$ with period π. The four data points represent six-photon count rates integrated over four days and normalized using single-photon count rates to account for coupling efficiency over time. Coincidence rates arising from higher-photon number terms or otherwise were not subtracted from the data. Error bars are given the standard deviation of detected events, assuming Poissonian statistics. Blue sinusoidal plot of near unit contrast is plotted as a guide.

pulsed down-conversion process that leads to different terms in the output state, allowing false heralded events: the eight-photon input $|4\rangle_b|4\rangle_c$ can give rise to the term $\frac{-i}{27\sqrt{3}}|2\rangle_i|3::2\rangle_{j,k}^{\pi/2}|1\rangle_l$ in the output state which in our experiment would be interpreted as a heralded "$|2\rangle_j|2\rangle_k$" event (see Supplemental Material [31]).

The heralded generation of path entanglement will be crucial to the practical application of quantum metrology; the schemes presented here are scalable to arbitrary large

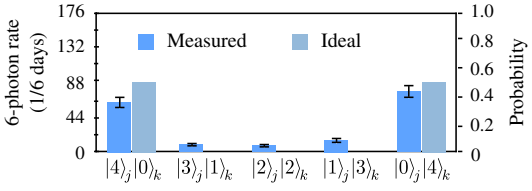

FIG. 4 (color online). Heralded generation of the $|40\rangle + |04\rangle$ state. The distribution of photon statistics from measuring a heralded four-photon NOON state. The sixfold detection rates are normalized by single-photon detection rates to account for relative source, coupling, and detection scheme efficiencies. Error bars are given the standard deviation of detected events, assuming Poissonian statistics.

entangled states [13,15]. States that are robust to loss will be particularly important. The integrated waveguide architecture delivers the high stability and compact implementation required for real world applications. In particular, integrated variable beam splitters [28] will allow optimization of quantum state engineering in the presence of loss [20,32]. The ongoing development of efficient number resolving detectors and deterministic photon sources such as single emitters or multiplexed down-conversion schemes [33], shows promise for practical quantum metrology and other photonic quantum technologies when combined with circuits such as that described here. Real time quantum metrology requires high repetition rate (bright) sources of many photons. Future development will also require integration of fast feedforward—using, for example, electro-optic materials—with the circuit demonstrated here to permit only intended quantum metrology states to interact with measured samples. This will likely form a building block for scalable generation of arbitrarily large entangled states [15,34].

We thank J. P. Hadden, A. Laing, A. Lynch, G. J. Pryde, J. G. Rarity, F. Sciarrino, A. Stefanov, and X. Q. Zhou for helpful discussion. This work was supported by EPSRC, ERC, IARPA, the Leverhulme Trust, PHORPBITECH, QAP, Q-ESSENCE, QIP, IRC, QUANTIP, and NSQI. J. L. O'B. acknowledges support through a Royal Society Wolfson Merit Award.

*Jeremy.OBrien@bristol.ac.uk

[1] N. Gisin and R. Thew, Nat. Photon. **1**, 165 (2007).
[2] T. D. Ladd, F. Jelezko, R. Laflamme, Y. Nakamura, C. Monroe, and J. L. O'Brien, Nature (London) **464**, 45 (2010).
[3] V. Giovannetti, S. Lloyd, and L. Maccone, Science **306**, 1330 (2004).
[4] E. Knill, R. Laflamme, and G. J. Milburn, Nature (London) **409**, 46 (2001).
[5] J. L. O'Brien, Science **318**, 1567 (2007).
[6] S. Gasparoni, J. W. Pan, P. Walther, T. Rudolph, and A. Zeilinger, Phys. Rev. Lett. **93**, 020504 (2004).
[7] R. Okamoto, J. L. O'Brien, H. F. Hofmann, T. Nagata, K. Sasaki, and S. Takeuchi, Science **323**, 483 (2009).
[8] X. H. Bao, T. Y. Chen, Q. Zhang, J. Yang, H. Zhang, T. Yang, and J. W. Pan, Phys. Rev. Lett. **98**, 170502 (2007).
[9] Q. Zhang, X. H. Bao, C. Y. Lu, X. Q. Zhou, T. Yang, T. Rudolph, and J. W. Pan, Phys. Rev. A **77**, 062316 (2008).
[10] C. Wagenknecht, C. M. Li, A. Reingruber, X. H. Bao, A. Goebel, Y. A. Chen, Q. Zhang, K. Chen, and J. W. Pan, Nat. Photon. **4**, 549 (2010); S. Barz, G. Cronenberg, A. Zeilinger, and P. Walther, *ibid.* **4**, 553 (2010).
[11] R. Prevedel, G. Cronenberg, M. S. Tame, M. Paternostro, P. Walther, M. S. Kim, and A. Zeilinger, Phys. Rev. Lett., **103**, 020503 (2009); W. Wieczorek, R. Krischek, N. Kiesel, P. Michelberger, G. Toth, and H. Weinfurter, *ibid.* **103**, 020504 (2009).

[12] H. Lee, P. Kok, N. J. Cerf, and J. P. Dowling, Phys. Rev. A **65**, 030101 (2002).
[13] P. Kok, H. Lee, and J. P. Dowling, Phys. Rev. A **65**, 052104 (2002).
[14] J. Fiurasek, Phys. Rev. A **65**, 053818 (2002).
[15] H. Cable and J. P. Dowling, Phys. Rev. Lett. **99**, 163604 (2007).
[16] F. Mayinger and O. Feldmann, *Optical Measurements: Techniques and Applications* (Springer, New York, 2002), 2nd ed..
[17] A. Abramovici, W. E. Althouse, R. W. P. Drever, Y. Gursel, S. Kawamura, F. J. Raab, D. Shoemaker, L. Sievers, R. E. Spero, K. S. Thorne, R. E. Vogt, R. Weiss, S. E. Whitcomb, and M. E. Zucker, Science **256**, 325 (1992).
[18] K. Goda, O. Miyakawa, E. E. Mikhailov, S. Saraf, R. Ad- hikari, K. McKenzie, R. Ward, S. Vass, A. J. Weinstein, and N. Mavalvala, Nature Phys. **4**, 472 (2008).
[19] J. P. Dowling, Contemp. Phys. **49**, 125 (2008).
[20] R. Demkowicz-Dobrzanski, U. Dorner, B. J. Smith, J. S. Lundeen, W. Wasilewski, K. Banaszek, and I. A. Walmsley, Phys. Rev. A **80**, 013825 (2009).
[21] M. W. Mitchell, J. S. Lundeen, and A. M. Steinberg, Nature (London) **429**, 161 (2004).
[22] P. Walther, J. W. Pan, M. Aspelmeyer, R. Ursin, S. Gasparoni, and A. Zeilinger, Nature (London) **429**, 158 (2004).
[23] T. Nagata, R. Okamoto, J. L. O'brien, K. Sasaki, and S. Takeuchi, Science **316**, 726 (2007).
[24] I. Afek, O. Ambar, and Y. Silberberg, Science **328**, 879 (2010).
[25] R. Okamoto, H. F. Hofmann, T. Nagata, J. L. O'Brien, K. Sasaki, and S. Takeuchi, New J. Phys. **10**, 073033 (2008).
[26] H. Kim, H. S. Park, and S.-K. Choi, Opt. Express **17**, 19720 (2009).
[27] A. Politi, M. J. Cryan, J. G. Rarity, S. Yu, and J. L. O'Brien, Science **320**, 646 (2008).
[28] J. C. F. Matthews, A. Politi, A. Stefanov, and J. L. O'Brien, Nat. Photon. **3**, 346 (2009).
[29] B. J. Smith, D. Kundys, N. Thomas-Peter, P. G. R. Smith, and I. A. Walmsley, Opt. Express **17**, 13516 (2009).
[30] C. K. Hong, Z. Y. Ou, and L. Mandel, Phys. Rev. Lett. **59**, 2044 (1987).
[31] See Supplemental Material at http://link.aps.org/supplemental/10.1103/PhysRevLett.107.163602 for further details on nondeterministic photon number resolving detection schemes used; photon coincidence counting logic used; theoretical treatment of state evolution inside the chip; the multiphoton down conversion source, and an example of the effect of higher photon number contributions.
[32] M. Kacprowicz, R. Demkowicz-Dobrzanski, W. Wasilewski, K. Banaszek, and I. A. Walmsley, Nat. Photon. **4**, 357 (2010).
[33] J. L. O'Brien, A. Furusawa, and J. Vuckovic, Nat. Photon. **3**, 687 (2009).
[34] H. Cable, F. Laloe, and W. J. Mullin, Phys. Rev. A **83**, 053626 (2011).